Marine and Petroleum Geology 164 (2024) 106726

Contents lists available at ScienceDirect

Marine and Petroleum Geology

journal homepage: www.elsevier.com/locate/marpetgeo

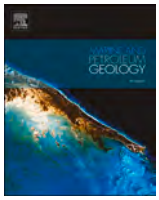

Seismic stratigraphy, stacking patterns and intra-clinothem architecture of a Late Holocene, Mud Wedge (Mediterranean Sea)

Giacomo Dalla Valle [a,*], Marzia Rovere [a], Claudio Pellegrini [a], Fabiano Gamberi [a]

[a] Istituto di Scienze Marine (ISMAR-CNR), Via Gobetti 101, 40129, Bologna, Italy

ARTICLE INFO

Keywords:
Continental shelf
Depositional processes
Delta-clinoform
Clinothem
Stratigraphy
Holocene
Unconventional reservoirs

ABSTRACT

Holocene inner shelf mud wedges are important paleoenvironmental archives because they typically contain continuous and extensive sedimentary sequences that can document past changes in sedimentary processes at very high temporal resolution. Here we investigate the fine-scale, seismic patterns of the Late Holocene Adriatic Mud Wedge (AMW), along the western Adriatic margin, to understand the processes of river-sea interactions and their effects on sediments distribution. While analyzing high-resolution seismic reflection profiles, we documented variations in the architectural stratal stacking patterns of the AMW, largely related to short-term fluctuations in sediment supply during the last sea level high (*ca.* 6000 years BP). Analysis of high-resolution seismic profiles revealed that the AMW consists of five clinothems (referred to here as "seismic units" SU1 to SU5) that were roughly dated by calibration with the continuous recovery well PRAD2-4. Each seismic unit is bounded by minor floodplains (H1 to H5), reflecting periods of relative sediment starvation at the margin. Our analysis provides an interpretative tool to differentiate the fluvial contribution of marine remodeling processes during the AMW evolution on millennium to centennial timescales. In addition, small-scale geomorphic features such as erosion surfaces, small distributary channels and terminal lobes were identified to provide information on heterogeneities that may impact an unconventional fine-grained delta reservoir, both in terms of continuity and overall hydrocarbon potential.

1. Introduction

From the beginning of the 1970s, the study of the sedimentary and facies architecture of modern delta-river systems improved significantly as the oil industry realized the enormous potential of hydrocarbon reserves within fossil deltaic systems (Wright and Coleman, 1973; for a thorough review, see Patruno and Helland-Hansen, 2018). In this context, Holocene systems can be studied with high resolution in order to generate predicting sequence stratigraphic models and scaling factors useful to characterize low-resolution datasets (Alexander et al., 1991; Martin et al., 1993; Xu et al., 2012). Holocene prodelta/mud wedge systems are composed, following the model by Van Wagoner et al. (1988) of a retrogradational Transgressive Systems Tract (TST) and an overlying, progradational High-stand Systems Tract (HST). In general, the HST-delta systems were mostly overlooked, as they were considered the result of a relatively simple, homogenous sedimentary bodies, consisting of repetitive stratigraphic patterns made up of advancing, prograding clinoforms during relatively stable eustatic conditions (Dıaz et al., 1996; Lobo et al., 2002). In the early 2000s, European research projects such as Eustrataform and Eurodelta investigated several dozens of meters thick prodelta systems extending over hundreds of kilometers seaward of major Mediterranean deltas (e.g. Hernández-Molina et al., 1994; Trincardi et al., 2004; Cattaneo et al., 2004; Bernè et al., 2007). These studies allowed the detailed reconstruction of the Late Holocene prodelta stacking patterns and of the relation between fluvial sediment supply and lateral transport along the coast, where the sediments can be further reworked by tides, waves, and oceanic circulation (e.g. Cattaneo et al., 2003, 2007; Traykovski et al., 2007; Drexler and Nittrouer, 2008; Harris et al., 2008; Pellegrini et al., 2015). In particular, the Late Holocene Adriatic Mud Wedge (AMW) has been intensively studied for the interplay between fluvial sediment supply and the along-shore, strong oceanographic regime (Oldfield et al., 2003; Cattaneo et al., 2003, 2004, 2007; Harris et al., 2008; Piva et al., 2008) (Fig. 1). These studies have been primarily focussed on the AMW evolution and architecture variability at the whole-body scale (Cattaneo et al., 2003, 2007; Niedoroda et al., 2005; Palinkas and Nittrouer, 2006, 2007; Harris et al., 2008). More recently, Pellegrini et al. (2021) concentrated the analysis on the Little Ice Age (LIA), just before widespread regulation and damming of

* Corresponding author.
E-mail address: giacomo.dalla.valle@bo.ismar.cnr.it (G. Dalla Valle).

https://doi.org/10.1016/j.marpetgeo.2024.106726
Received 31 August 2023; Received in revised form 15 January 2024; Accepted 21 January 2024
Available online 26 January 2024

Apennine rivers occurred.

The present study is based on the analysis of high-resolution seismic reflection profiles to decipher, in very high detail, the architecture of AMW by analyzing stacking patterns, and seismic facies distribution, as well as the presence of geomorphic elements within the AMW. The analysis allowed us to reconsider the interaction between the along- and across-shelf processes operating along the AMW and to compare it to other occurrences of inner-shelf, mud-wedges on both ancient and modern continental shelves at the sub-seismic scale. More specifically, we aim to: i) unravel the fine-scale geometry and internal architecture at the intra-clinothem scale, which are deposited at millennial to centennial timescales; ii) discuss the sedimentary processes that control the sediment deposition and dispersion across wide and low-angle inner continental shelves, and how these processes may be related to fluctuations in oceanographic regime and sedimentary inputs; iii) interpret the AMW fine-scale heterogeneities to aid in the interpretation of analog sedimentary systems developed in similar settings, both in ancient and modern successions.

2. The Adriatic Sea and the AMW: present-day physiography, sediment supply, and oceanographic setting

The Adriatic Sea is a semi-enclosed basin located in the central Mediterranean region, stretched between Italy and the Balkans (Fig. 1). The Adriatic Sea is connected with the Mediterranean Sea through the Otranto Strait, where water masses of both Atlantic and Levantine origin are exchanged between adjacent basins (Fig. 1). The Adriatic Basin is approximately 800 km long and 200 km wide elongated in NW-SE direction. The northern and central Adriatic sectors, located between the Po Delta and the Gargano Promontory, are shallow water (50–80 m of

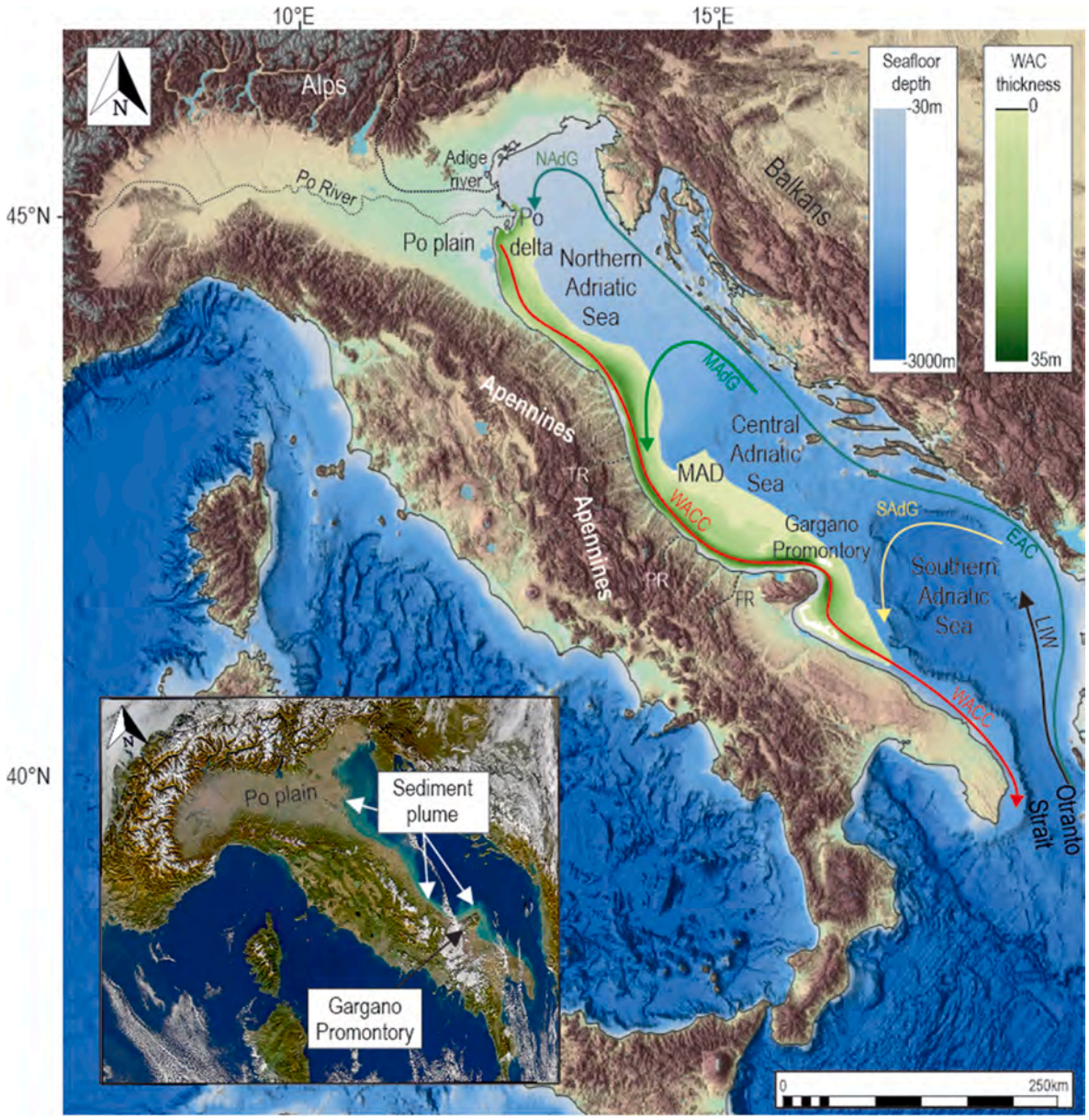

Fig. 1. Thickness distribution of the Late Holocene Adriatic high stand mud wedge (AMW) (Modified from Cattaneo et al., 2007). The bathymetry of the Adriatic Basin is from EMODnet data (https://emodnet.ec.europa.eu/geoviewer/). The pathways of the oceanographic currents flowing in the Adriatic basin are outlined: Western Adriatic Coastal Current (WACC), Eastern Adriatic Current (EAC), North Adriatic Gyre (NAdG), Mid Adriatic Gyre (MAdG), South Adriatic Gyre (SAdG), North Adriatic AdW (NAdDW), Levantine Intermediate Water (LIW) (redrawn with modifications from Poulain and Cushman-Roisin, 2001) The bottom-right inset is the true colour satellite image showing the WACC carrying the suspended sediment plume along the coast of Italy, from the Po Delta to the Gargano Promontory. Main Apennine Rivers, TR: Tronto River, PR: Pescara River, FR: Fortore River.

depth), with an almost flat seafloor, except for the Mid Adriatic Depression, that reach depths of 290 m (Trincardi et al., 2014). Freshwater is discharged into the Adriatic Sea from Alpine rivers (including the Po River) to the north, and Apennine rivers (e.g. Tronto and Pescara rivers) to the south. The Po is the largest Italian river, draining an area of 74,000 km^2 and with an average flow of 1500 m^3/s, and, collectively, Alpine rivers drain ~30% of the total catchment area of ca. 173,000 km^2. The Po, with 13–15 million tons per year (Mt/yr) is the largest single supplier of sediment to the Adriatic Sea (Cattaneo et al., 2003; Kettner and Syvitski, 2008). The relatively short, steep Apennine River account for around 32 Mt/yr, or about 60% of the sediment input to the Adriatic (Cattaneo et al., 2003). The AMW is a 600 km long mud-wedge, developed from the Po Delta to offshore Gargano Promontory in the inner sector of the Western Adriatic Shelf (Figs. 1–3). The AMW is currently swept by the surficial Western Adriatic Coastal Current (WACC) which carries fresh water and suspended sediments running shore-parallel to the Italian coast, with flow velocities of ca. 30 cm/s that guarantee an overall southward transport (Poulain, 2001) (Fig. 1). Besides, the across-shelf sediment transport is very limited, due to the confinement effect of a strong haline front (Orlic et al., 1992; Artegiani et al., 1997). This oceanographic setting is responsible for the great elongation of the AMW together with its limited cross-shelf extent (Cattaneo et al., 2007; Harris et al., 2008). The AMW has a simple, delta-clinoform morphology, with a submerged topset and with the bottomset that reaches depths of 60 m (Cattaneo et al., 2007; Pellegrini et al., 2015, 2020) (Fig. 2a and b). Only offshore Gargano Promontory the simple wedge-shaped geometry becomes more complicated, as the AMW is split into two components by the presence of an outcropping basement (Cattaneo et al., 2007; Pellegrini et al., 2015) (Fig. 2b). The AMW deposition began ca. 6 kyr BP, during the current High-Stand period of sea level (Trincardi et al., 1994; Cattaneo et al., 2003) (Fig. 2c).

3. Data and methods

3.1. Data analysis

This study is based on a dataset of high-resolution CHIRP seismic sonar profiles, acquired on board the R/V Urania during the 2000s (COS_2000, CSS_2001, and KS_2002 cruises) with a 16-transducer hull-mounted Teledyne Benthos III sound source and 2–7 kHz signal capable of penetrating the sedimentary succession for dozens of meters. Due to the large regional extent, we sub-divided the AMW into three sectors: the northern sector, between Conero Promontory and the Tronto River, the central sector which comprises the Pescara River and the Punta Penna Promontory, and the southern sector, offshore the Gargano Promontory (Fig. 3a and b). The seismic profiles have been interpreted following these steps: 1) identification of intra-AMW reflectors (H1 to H4) that are traceable along the entire mud wedge through manual picking and software (Geosuite All Works) aided correlation in order to divide the AMW into discrete clinothems (labeled as Seismic Units, SU1-SU5) (Fig. 4 a-f; 2) generation of isopach maps (all the depths are in ms) for each clinothem through Global Mapper software using a grid of 2 km × 2 km (Fig. 5a–f). Successively, clinothems have been characterized by studying their internal geometries, variations in seismic facies characters, and stacking patterns, and by identifying their bedset terminations (Figs. 6 and 7). Chronostratigraphic subdivision of the clinothems within the AMW relies only on the correlation of the individual bounding reflectors (H1 to H4) to the reference borehole PRAD 2-4, collected within the EU project PROMESS 1 (Bernè et al., 2007) (Fig. 2c)., Borehole PRAD 2-4 yielded a continuous, 35 m long sediment recovery, collected on the inner shelf of the Western Adriatic Sea, through a very expanded section across the Late Holocene. Vigliotti et al. (2008) presented a description of the few control points used in generating the age-depth model of the PRAD 2-4 borehole (Fig. 2c).

3.2. Clinothems in the chronostratigraphic framework

Clinothems from SU1 to SU5 are bounded by well-defined, high-amplitude horizons, named: maximum flooding surface (Mfs), H1, H2, H3, H4, and the present-day seafloor (Fig. 2c, 4a-f). The boundary horizons H are highlighted by downlap terminations and bound relatively conformable strata, and, presumably, mark short-lived episodes of relative sediment starvation between successive pulses of high sediment accumulation. Since during the Late Holocene the Adriatic shelf does not experienced meter-scale variations in accommodation space, it remains difficult to document a shoaling-upward trend within the AMW, even by studying changes in the fauna association (e.g. Piva et al., 2008); however, the AMW overall represents the Highstand System Tract characterized by an overall progradational/aggradational character.

The age span of the SUs of the AMW was calculated from the chronology of the borehole PRAD2-4 for the Late Holocene with few control points through a ca. 12 m thick HST succession (Vigliotti et al., 2008). Based on the PRAD2-4 borehole, the SU1 encompasses a period from ~5700 kyr BP to ~3200 kyr BP (Fig. 2c). The SU2 is between H1, at the base, and H2, at the top, which spans approximately between ~3.2 kyr and ~1000 yr BP (Fig. 2c). The SU3 rests between H2, at the base, and H3 at the top. SU3 spans between ~1000 and 800 yr BP (Fig. 2c). SU4 is bounded between the H3 and the H4 reflectors which matches the base of the Little Ice Age (LIA; Piva et al., 2008). The SU5 encompasses the last ~550 years, as it is bounded at the base by the LIA (H4) and the present-day seafloor at the top (Fig. 2c).

4. Results

4.1. The Late Holocene adriatic mud-wedge

The present-day seafloor gradient of the AMW is exceptionally low in the northern sector but progressively becomes higher in the central sector, with maximum values around the Gargano Promontory (Fig. 3a).

The Maximum flooding surface (Mfs), created by manually picking the Mfs reflectors all along the investigated AMW sectors shows similar slope gradient with no remarkable differences with respect to the present-day seafloor gradient of the AMW (Fig. 3b). A time-lapse of the progressive AWM construction, created by picking the key boundary horizons (H1–H4), shows as the thickening of bottomset is almost negligible, as the majority of sediments are stored in the topset and the upper foreset regions (Fig. 4a–f). The AMW isopach map, created by picking the Mfs and the seafloor reflectors, shows that the thickness of the mud belt increases southward: the overall values range between 20 and 25 ms for the northern and central sector, whereas the Gargano Promontory hosts the major depocenter (up to 35–40 ms thick) (Fig. 5a). The Gargano depocenter displays a strike-elongated (sub-parallel to the present-day coastline) orientation, with a smooth top surface (Fig. 5a). Internally, the AMW is composed of discrete clinothems generally form a forestepping, sigmoidal, progradational pattern, migrating skewed compared to the sediment entry points (Figs. 6 and 7).

4.1.1. Clinothem SU1

Bounded by the Maximum flooding surface (Mfs) and the Horizon 1 (H1), the clinothem SU1 represents the initial stage of the AMW deposition after the attainment of the maximum marine ingression (Fig. 4b). The SU1 reaches a maximum thickness of 9 ms in the northern sector and of 13 ms offshore Gargano Promontory, where an elongated, smooth depocenter parallel to the coast is present (Fig. 5b). However, the SU1 topset and the upper foreset are characterized by widespread biogenic gas blanketing the seismic signal, therefore there is uncertainty about the SU1 maximum thickness which could be increased by a few ms (Fig. 4b and 5b). Southward of the Conero Promontory, the SU1 thickness appears uniform, whereas a series of localized, sediment accumulations is present in front of the Tronto River mouth and in the offshore sector between Pescara River and Punta Penna Promontory (“isolated

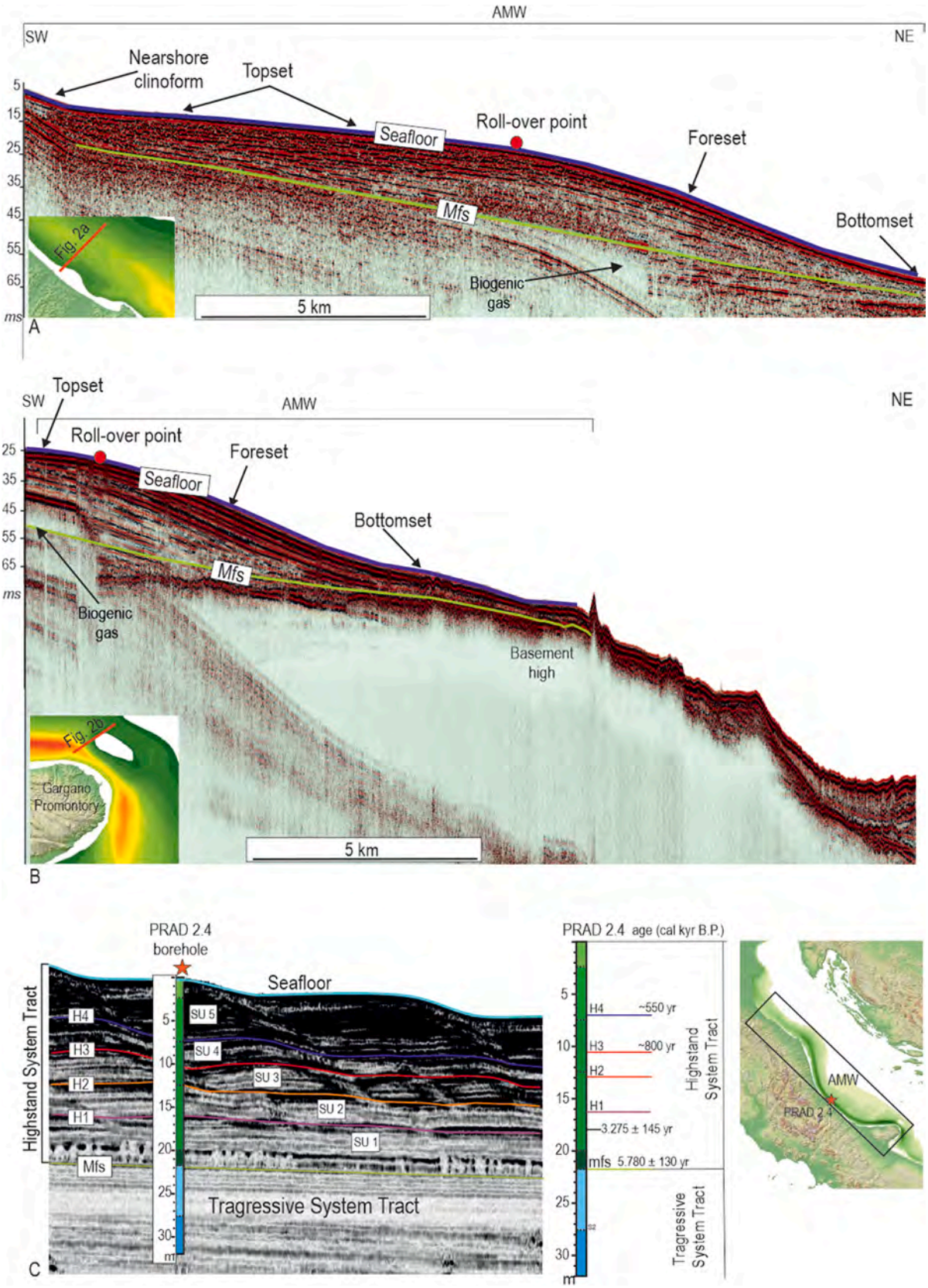

Fig. 2. Seismic reflection profiles CHIRP, vertical resolution of ca. 0.4 m, (see the inset boxes for their geographic location) showing the internal architecture and the main physiographic elements of the AMW, in (a) the northern sector and (b) the southern sector. Green horizon marks the maximum flooding surface (*Mfs*) at the base of the AMW. Purple horizon matches the present-day seafloor. c) Internal subdivision of the AMW into distinct clinothems (Seismic Unit, SU) by the 4 key horizons (H1–H4) roughly dated by correlation with the PRAD 2-4 borehole, which provides the chronostratigraphic framework (Map in inset bottom right for the location of the PRAD 2-4 borehole along the AWM).

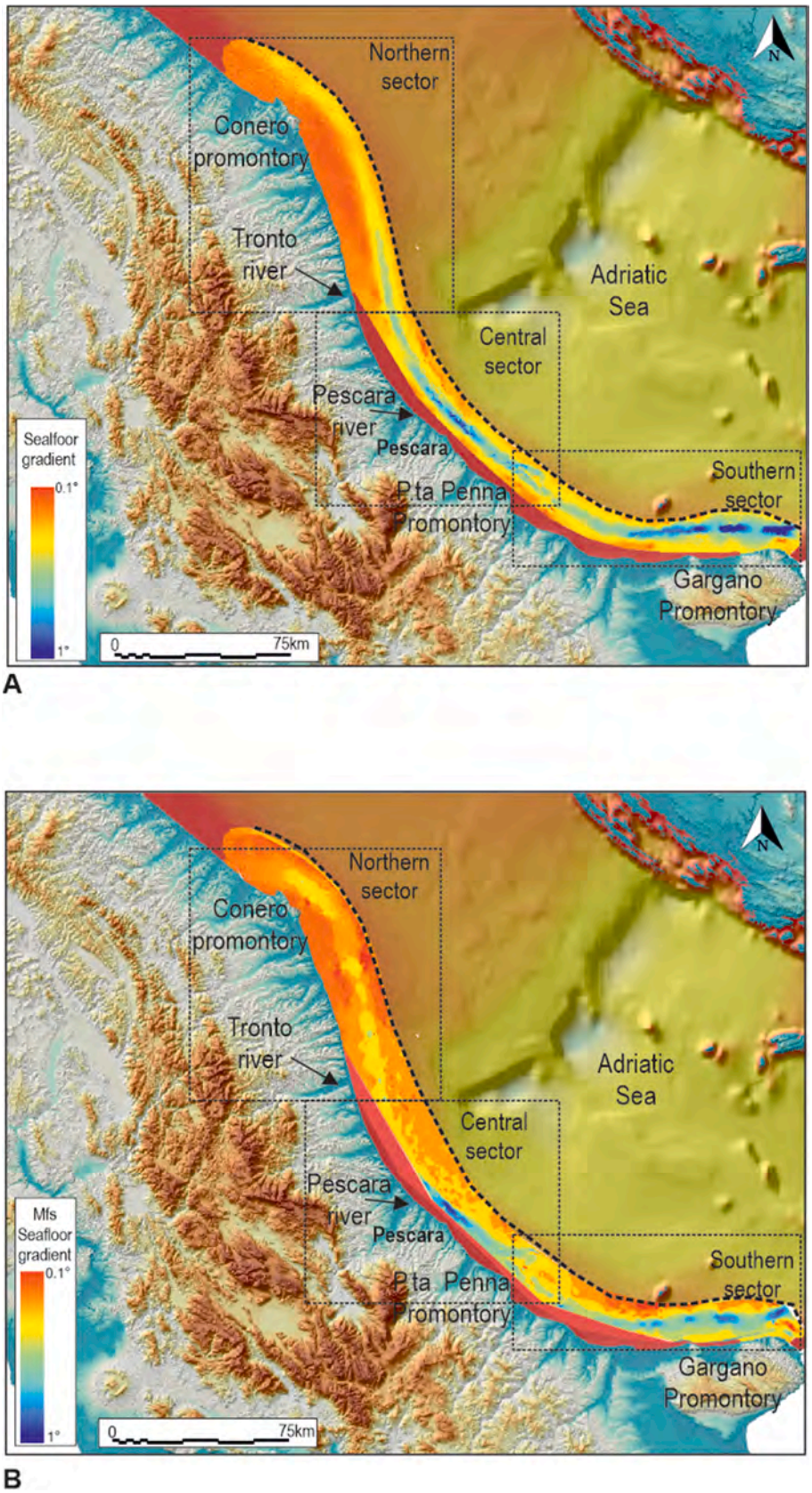

Fig. 3. Slope gradient of (a) the present-day seafloor and (b) the maximum flooding surface (*Mfs*) created by picking the two reflectors corresponding to *Mfs* and seafloor, and then interpolated with Global Mapper and Allworks Geosuite software packages. The lack of data due to the presence of gas blanketing the seismic signal of CHIRP profiles affects the reliability of the *Mfs* gradient in the central-southern sector. Note how the two surfaces have very similar gradients, in particular in front of the Pescara River and offshore the Gargano Promontory. Dashed line: offshore limit of the examined AMW area.

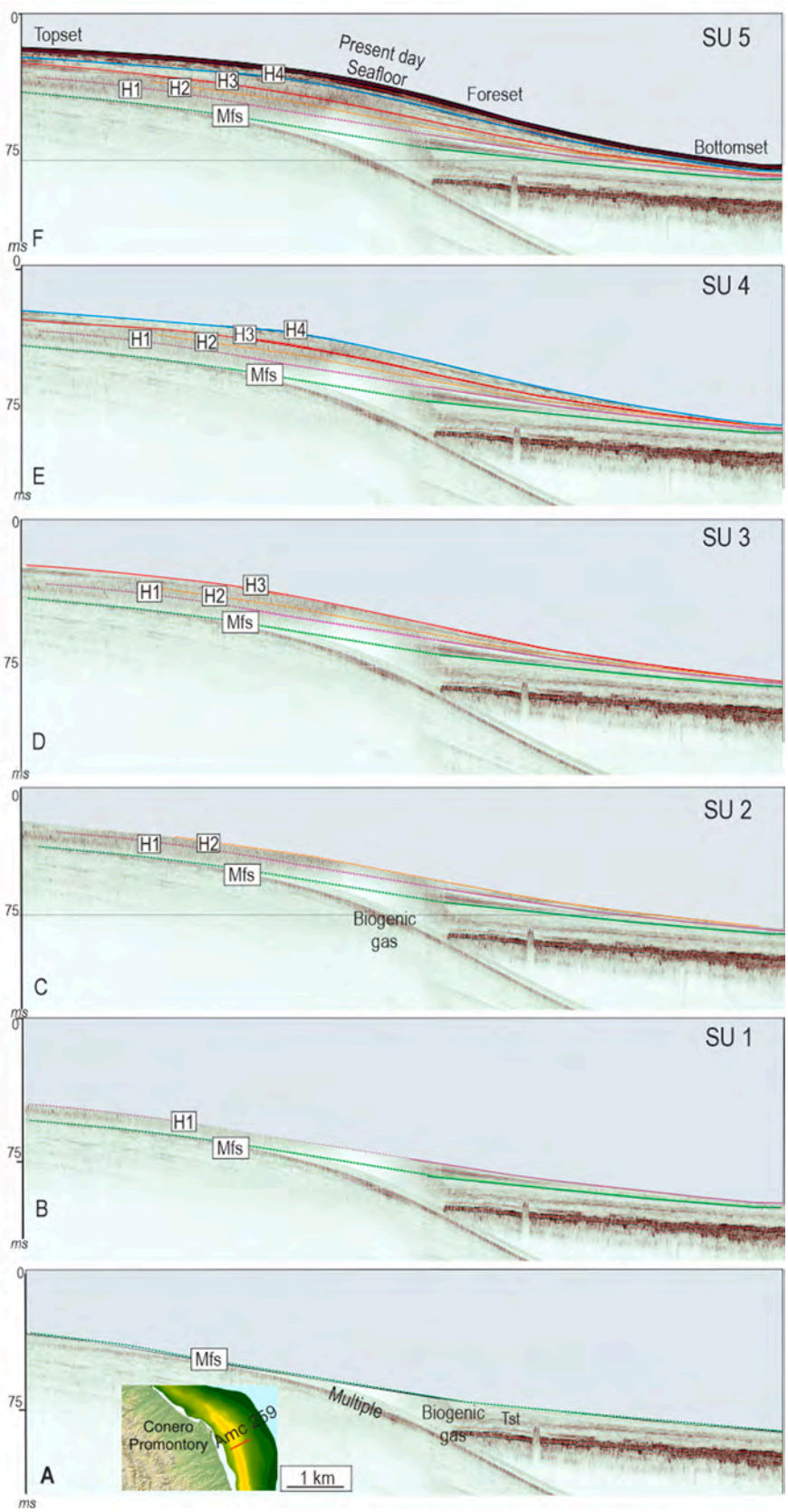

Fig. 4. Time-lapse of the AWM evolution with its constitutive five seismic units (SU1–SU5) and their boundary horizons (H1–H4/Seafloor). The relative change in the depth of the seafloor during the AMW evolution can be appreciated, and in particular the fact that the majority of the sedimentation occurs in the area between the topset and the upper foreset, while the bathymetry in the bottomset region remains almost unchanged.

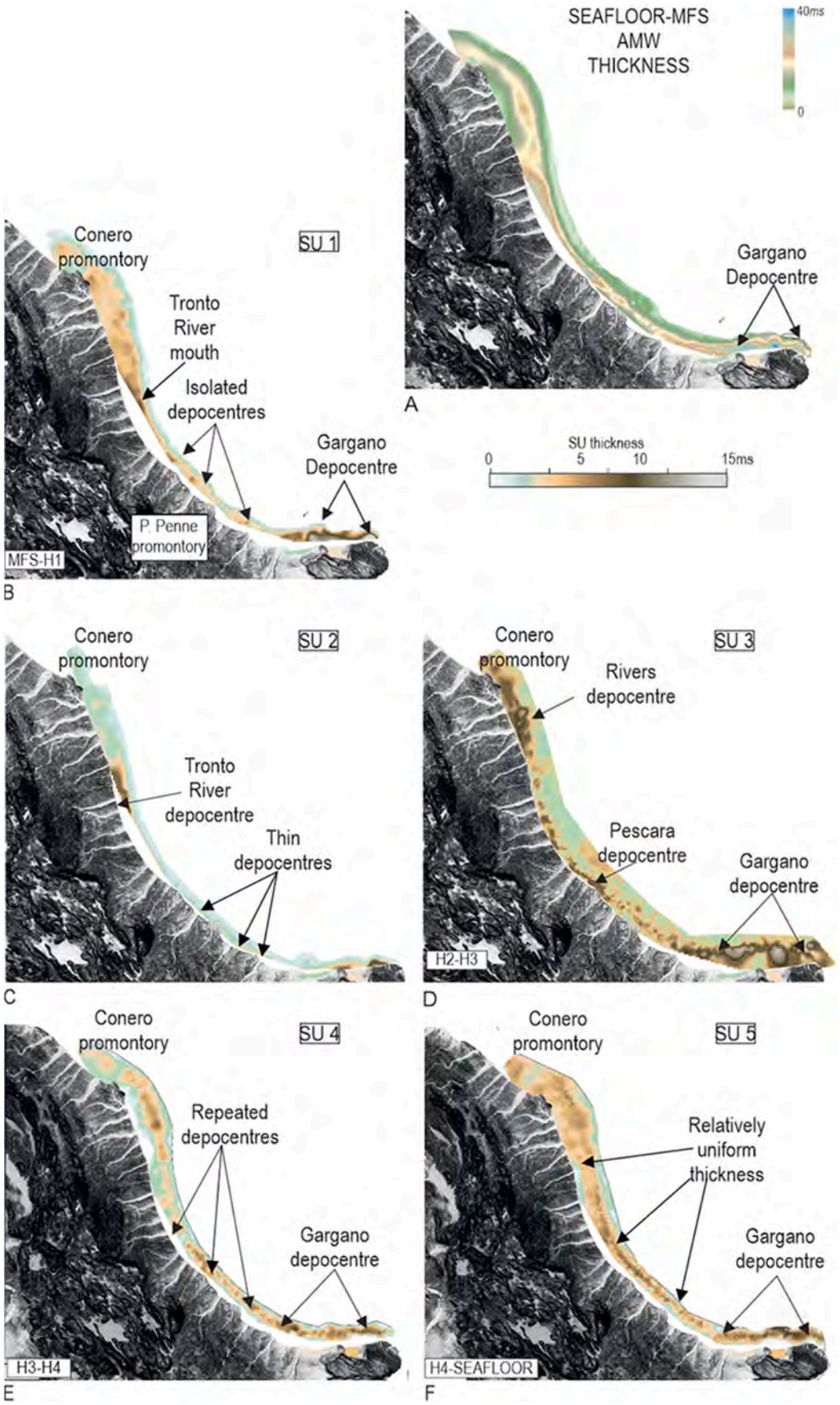

(caption on next page)

Fig. 5. Isopach maps of (a) the whole AMW and of its constituent clinothems SU1 to SU5 (b–f). Note that a persistent depocenter is maintained throughout the entire construction of the AMW only in the offshore Gargano Promontory. A strengthening of WACC along-coast current, which is increasingly capable of reworking river-derived deposits as the AMW grows, may be indicated along the other AMW sectors by the progressive transition from localized, repeated sediment depocentres to more smoothed and elongated depocentres.

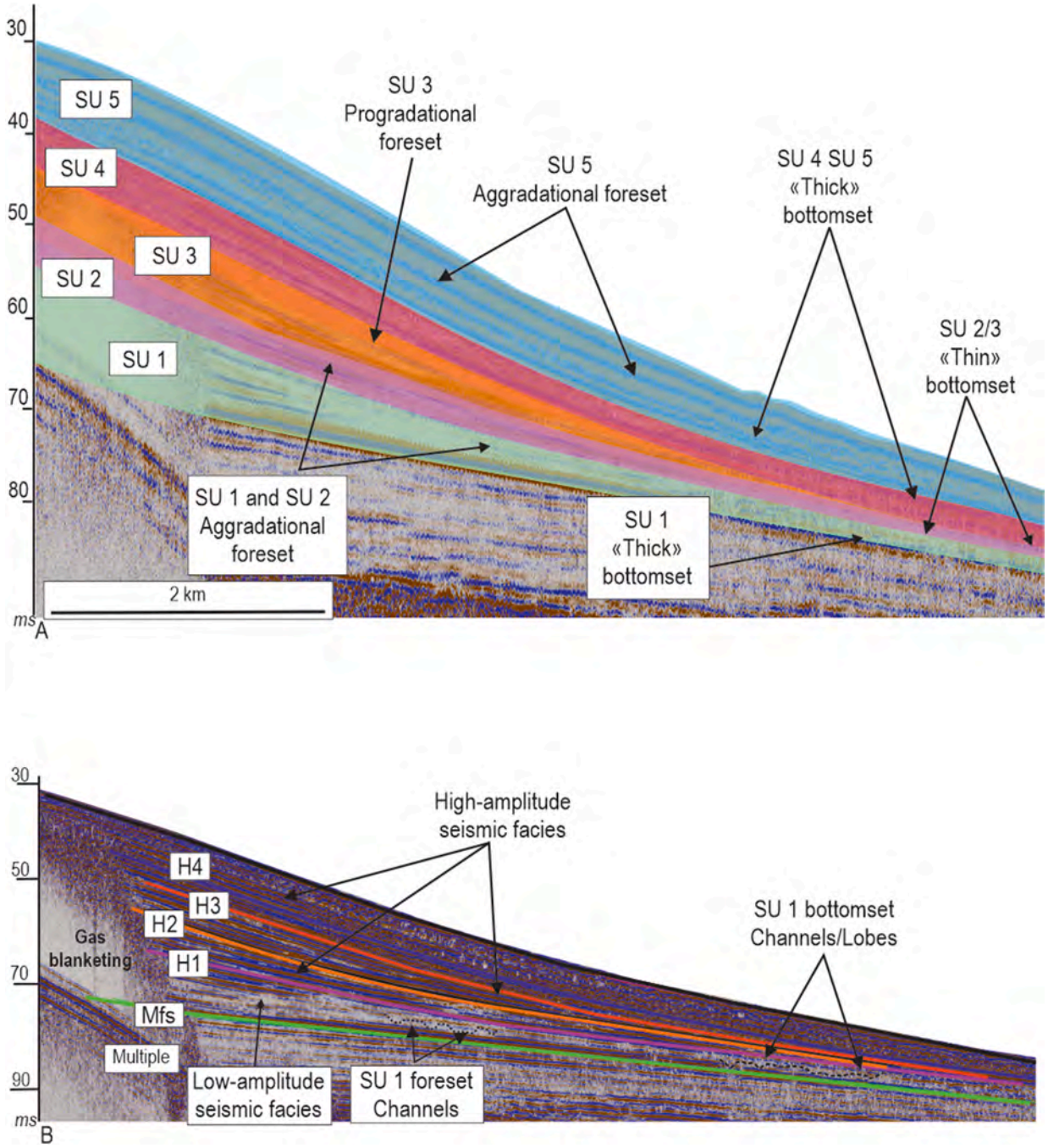

Fig. 6. a) Colour sketch of the seismic units (SU) showing the external geometry of each clinothem of the AMW clinoform, highlighting, in particular, the differences between the foreset character and the thick and thin bottomset classification. b) Example of across-shelf profile shows distinct sigmoidal clinothem geometries, bounded by the key horizons described in the text. Note the abrupt termination of SU3, which represents the clinothem with the shortest offshore extent. The Irregularities in the otherwise well-bedded, high-amplitude reflectors along the foreset may represent channel-like incisions, whereas channel-lobe deposits seem to be present in the distal bottomset. See Fig. 8b and 8c for a more detailed characterization of these geomorphic elements.

depocenters" in Fig. 5b). When viewed along dip, the SU1 has a marked aggradation both along the foreset and in the bottomset (thick bottomset type) (Fig. 6a and b). The SU1 has seismic facies characterized by low-amplitude, continuous reflections, that are slightly convergent basinward into high-amplitude seismic facies (Figs. 6b and 7a). The intra-clinotheme, stacked bedsets are arranged into a series of downlap, which results in an overall progressive landward migration (Fig. 7a). In across- and along-shore oriented profiles the foreset is characterized by V-shaped incisions that are up to 500 m wide and with depths of 5–8 ms (Fig. 6b and 8a, b). Incisions are interpreted as due to the presence of

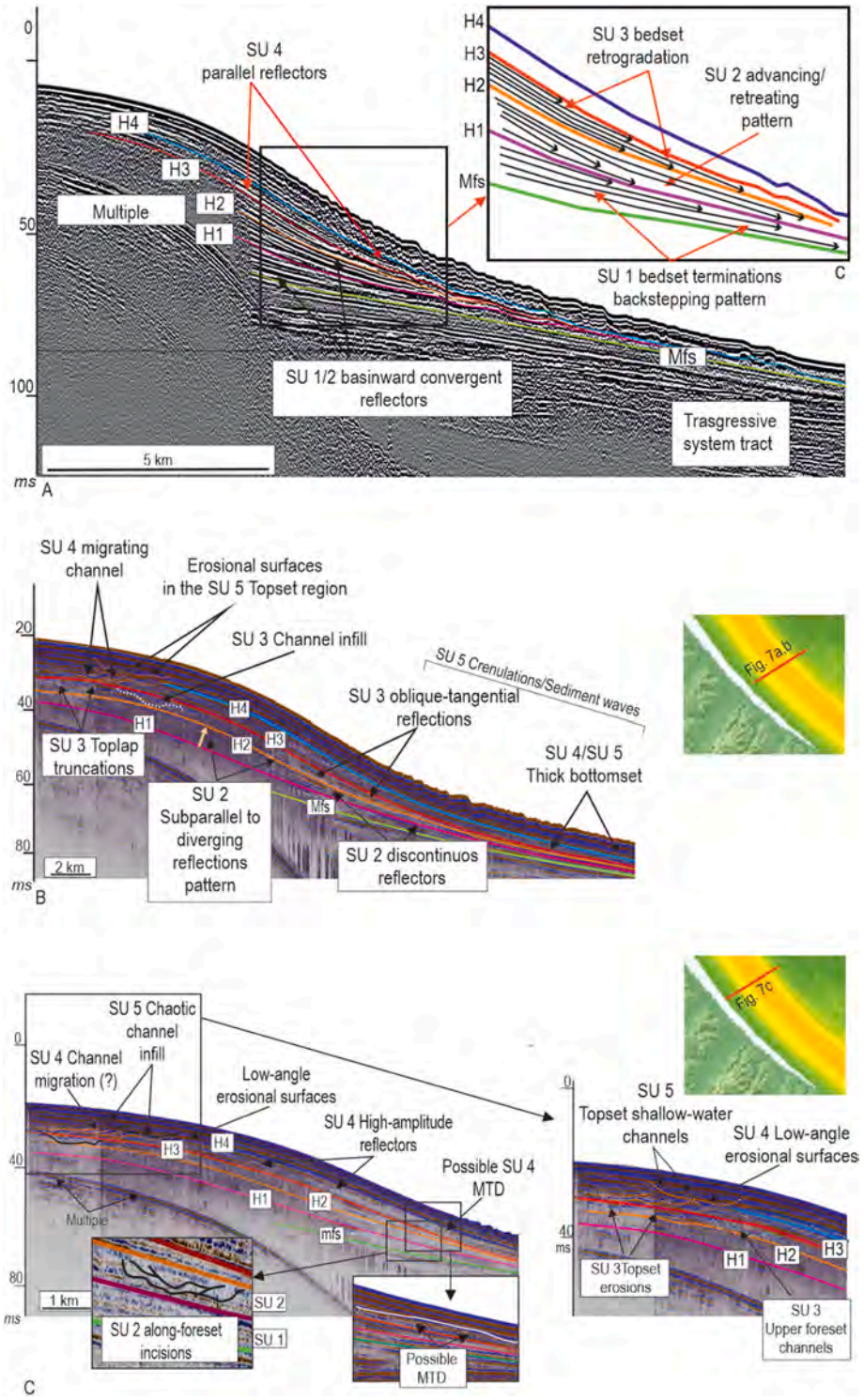

Fig. 7. a) CHIRP profile showing the stratigraphic stacking patterns of the different SUs and the reflectors arrangement of the clinothem foreset region. The upper-right inset shows a zoom of intra-clinothem, progradational/retrogradational bedset terminations, which are possibly related to short-time variations of sedimentary inputs and/or changes in the along-shore current intensity b) Details of the seismic facies character of SU1, SU2 and SU3 with outlined the fine-scale arrangement of the reflector architecture, and the main geomorphic elements in the topset region of SU4/5 c) Particular of the topset-forest region, showing the presence of incisions also along the SU2 resembling the presence of channels scouring the foreset. The SU4 unit shows uniform thickness along both the foreset and bottomset, whereas the SU5 unit shows U-shaped erosional surfaces on which multiple, shallow-water, migrating channels develop. A chaotic thin interval seems to witness the presence of a mass-transport deposit within the SU4. The lower right inset represents a zoom in the topset region in Fig. 7c, showing in more details the presence of shallow-water, erosional channels encased in low-angle, large erosional surfaces both in the SU4 and SU5 topsets.

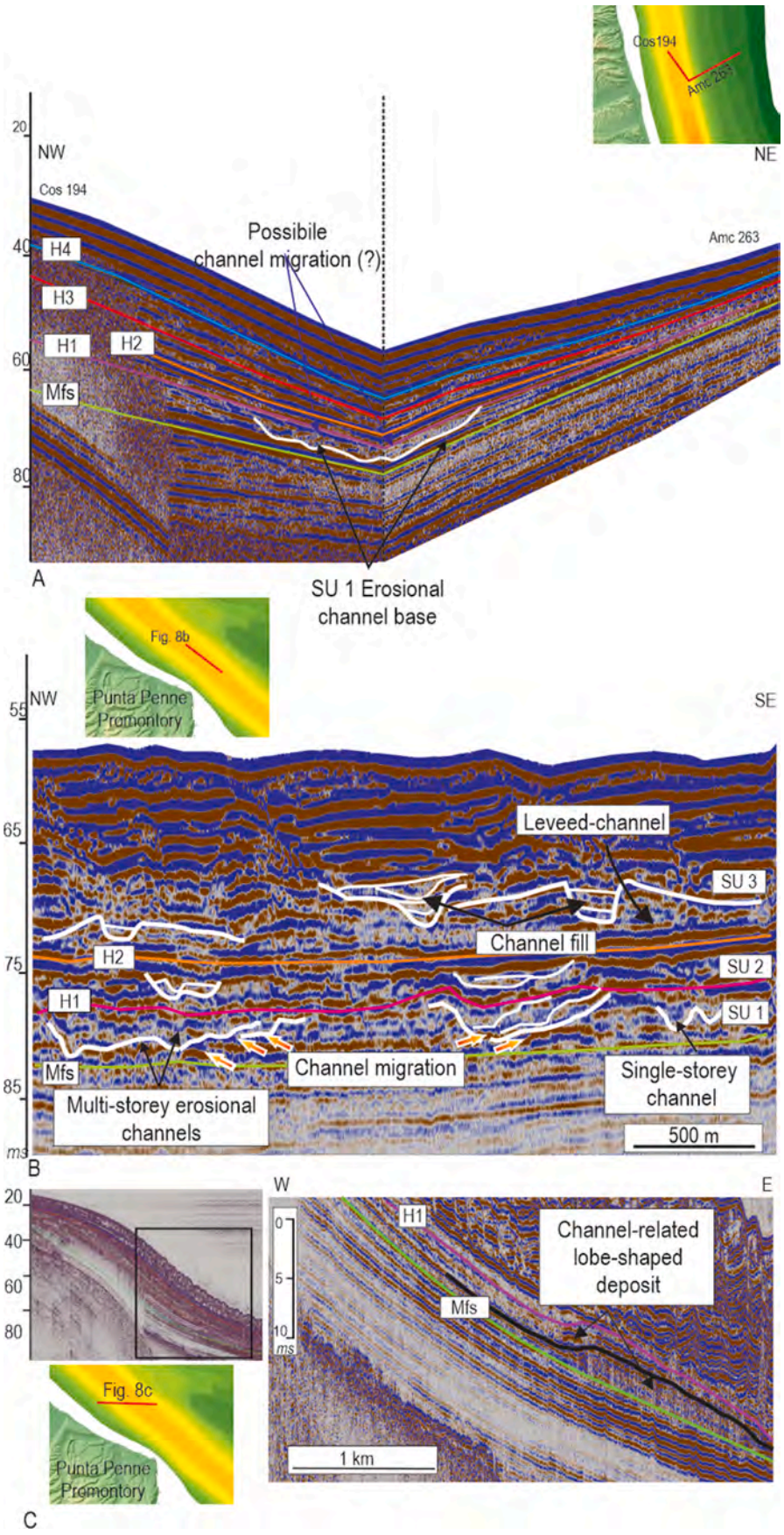

(caption on next page)

Fig. 8. a) Cross correlation of seismic CHIRP profiles showing the possible presence of erosive channels along the foreset and bottomset of SU1 in the AMW northern sector. b) Channels in the SU1 and SU2 units seem to have an erosional character, whereas channels in the SU3 unit seem associated to depositional levees. Examples of single-storey channels, with fixed position or limited displacement vs multi-storey channels which have characters suggesting important channel mobility, possibly associated with migrations c) Particular of the distal foreset/bottomset region, where seismic mounds, interpreted as distal frontal splays/terminal lobes, are present at the SU1 channel terminations.

very small-scale, shallow-water channels that scour the topset (which is actually not visible due to gas hampering), the foreset, and that can probably reach the bottomset (Fig. 8a). Channel-infill shows seismic facies that seems to resemble fine-grained lithology, mud or silt with minor sand (Fig. 8a and b). Channels also develop terminal frontal-lobes in the distal foreset, with thickness less than 10 ms, as a series of mound-shaped deposits with seismic chaotic facies witnesses (Fig. 6b and 8c).

4.1.2. Clinothem SU2

The clinothem SU2 (Fig. 4c) has a thickness that increases moving southward, from an average of 8 ms off the Conero Promontory to values of 11 ms offshore the Gargano Promontory (Fig. 5c). The isopach map shows a pronounced depocentre in the northern sector, offshore Tronto River, and an another one in the Gargano offshore, with scarce, thin accumulation sectors around the Punta Penne offshore ("thin depocenters" in Fig. 5c). Geometrically, the SU2 shows progradation and aggradation along the foreset and with a thinner bottomset, compared to SU1 (thin bottomset type) (Fig. 6a and b). Internally, the clinotheme is arranged into a series of marine onlap terminations which highlight basinward to landward the terminations of the bedsets (Fig. 7a). The foreset seismic facies has high-amplitude reflectors, with scarce continuity, showing sub-parallel to converging pattern (Fig. 7b). As for the SU1 case, especially offshore Pescara-Punta Penne coastal sector, the foreset uniformity is interrupted by a series of small-scale, V-shaped incisions (Fig. 7c). These features are interpreted also in this case as erosive, shallow-water distributary channels, crossing the foreset down to the bottomset (Fig. 7c and 8b).

4.1.3. Clinothem SU3

The isopach map of the SU3 clinothem shows that the thickest accumulation takes place offshore Gargano Promontory, with an elongated depocentre about 8 ms thick (Fig. 5d). Others two main depocenters are present in front of the rivers south of the Conero Promontory, and the Pescara River mouth (Fig. 5d). The SU3 unit shows marked aggradation along the upper foreset and rapid decrease in thickness in the bottomset (thin bottomset type) and an abrupt offshore termination (Fig. 6a and b). The stratal stacking pattern delineates a series of bedset terminations that give rise to an overall back-stepping architecture (Fig. 7a). The topset is characterized by many toplap truncations suggesting the presence of erosional surfaces, 1–2 km wide (Fig. 7b). Within these erosional surfaces, channels seem to be present and are in some cases filled by sediments (Fig. 7b). Along the upper foreset, distributary channels are present and their character is sometimes depositional, as they seem to developing very thin levee deposits (less than 5 ms thick) on their sides (Fig. 8b).

4.1.4. Clinothem SU4

Compared to previous SUs, the isopach map of the SU4 shows a uniform thickness along all the AMW, with closely-spaced, lobated deposits ("repeated depocentres" in Fig. 5e). The SU4 average thickness is around 5 ms, except for the thickest depocenters located offshore Gargano Promontory (Fig. 5e). Across-dip, it shows a relatively uniform thickness moving offshore, with aggradational foreset and bottomset (thick bottomset type in Fig. 6a and 7b). Along the foreset, the reflectors show a high-amplitude facies, and are parallel and well-bedded, as channels or incisions are not present (Figs. 6b and 7a, b). On the contrary, wide, low-angle, erosional surfaces are visible in the topset region, as witnessed by many toplap truncations (Fig. 7b and c). As for the previous SU3, also in this case, topset channels are enclosed within the wider erosional surfaces (Fig. 7c). Southward of the Conero Promontory, the seismic facies of the lower foreset is locally chaotic and stands out from the otherwise undisturbed upper foreset stratigraphy, made up of well-bedded, high-amplitude reflections (Fig. 7c). This chaotic facies may correspond to sediment failure that have involved a thin package of sediments (Fig. 7c).

4.1.5. Clinothem SU5

Also, in the SU5 a southward increase in thickness is observed, with the sedimentary pile that reaches values of 12 ms offshore Gargano Promontory (Fig. 5f). Sediment distribution appears rather uniform along the northern and central sectors, with the presence of elongated and coalescent depocentres (Fig. 5f). The SU5 has a marked progradational and aggradational character along the foreset and the distal bottomset, respectively (thick bottomset type) (Fig. 6a, b, 7a). The topset region represents the thicker sector of the whole clinothem, with the abundant presence of shallow-water channels, resting on top wider, low-angle erosional surfaces, around 5–7 ms deep (Fig. 7b and c). Generally, the incisions end in the upper foreset, where, when see along-dip, display bidirectional downlaps that may resemble crevasse deposits or small-scale delta lobes (Fig. 9). Wavy reflections affect the foreset and bottomset (Figs 7b). Wavy reflections (crenulations in the sense of Urgeles et al., 2011) display overly complex geometric patterns when viewed along strike, as they are also cut by subtle, low-angle erosional surfaces matching with truncated reflections, that seem to resemble large scours (Fig. 9).

5. Discussion

5.1. The Late Holocene AMW: thickness and sediment distribution

Along continental margins, multiple rivers feed the shelf and their sediment contributions combine together to form a line source (Jaeger and Nittrouer, 1999; Walsh et al., 2004; Cattaneo et al., 2007; Liu et al., 2009; Patruno et al., 2015; Pellegrini et al., 2021). Sediments originate from the mouth of each river, but along the shelf these contributions become mixed together by waves and currents (Warrick, 2020), in a way that distinct compositional fingerprints of the fluvial catchments need to be determined to understand sediment provenance (Revel et al., 2010; Ehrmann et al., 2016). This is particularly true in muddy systems affected by advective sediment transport, such as those associated with the Rhone, Mekong, Yellow and Yangtze rivers. Here the sediments delivered to the sea remain confined in the inner shelf along mud banks that extend for 150 km (Bernè et al., 2007), 500 km (Xu et al., 2012), 600 km (Liu et al., 2009) and up to 800 km (Liu et al., 2009), respectively.

In the case of the AMW, the isopach maps show that SU1, SU2, and SU3 host localized depocenters that protrude from the coast in a lobate shape, and are located in particular between Conero Promontory and Tronto River and offshore the Pescara River (Fig. 5b, c, d). We interpret these localized lobes as features of high-discharge flooding from the Apennine Rivers. We assume that, during the interval between SU1 and SU3 deposition, the cross-shore sediments transport was an important component of the sediment budget delivered to the inner-shelf, while the sediments were not efficiently redistributed along the shoreline (i.e. by the action of the WACC). With the further progressive mudbelt progradation and aggradation, and the consequent reduction in bathymetry and accomodation space (Fig. 4a–f), there is a progressive overturning in the style of deposition, with the along-shore currents taking over in the

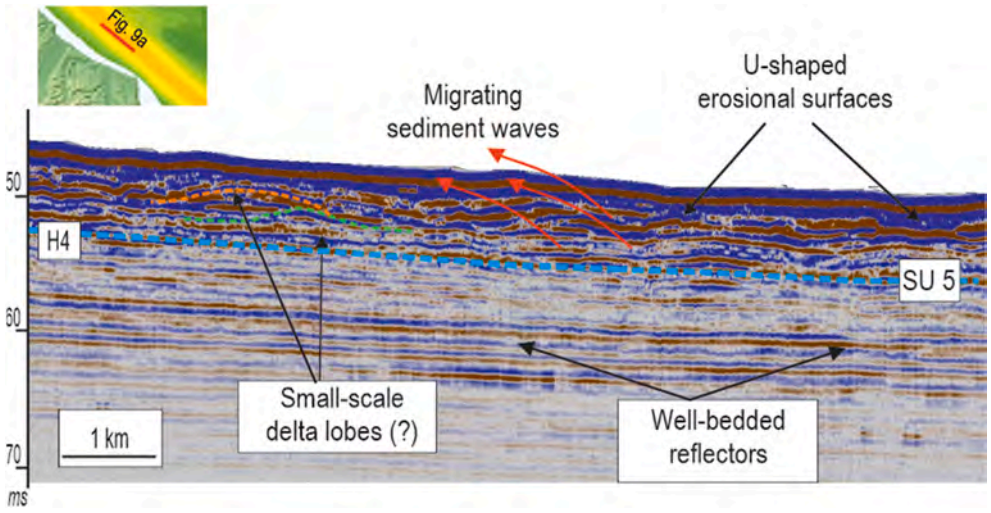

Fig. 9. Evidence of small-scale lobes in the upper foreset region of the SU5 unit around Punta Penna. The stratigraphic architecture of the older SUs is characterized by continuity of the reflectors along the foreset, whereas in the later stages as SU5, the presence of sediment waves and depositional lobes arranged in a compensational-cycle style, may be related to a more complex interaction between riverine inputs and along-shore currents.

redistribution of the sediments along the AMW.

During the entire AMW development, the Gargano depocenter remains a long-lived feature, appearing as an elongated, smooth and thick depocentre (Fig. 5a–f). We hypothesize that such depocentre architecture is the result of the accelerated hydrodynamic regime created by the interaction between the WACC and the coastal bulge formed by the Gargano Promontory (see Cattaneo et al., 2007; Martorelli et al., 2010). The region upstream the Gargano Promontory tip represents, in fact, a coastal sector where a substantial reduction of the along-shore current velocities has been observed (e.g. Harris et al., 2008), and this regime can lead to an increased sediment deposition, with the Gargano depocentre representing the thickest AMW portion.

5.2. Geometry of the SU: offshore extent and bottomset type

The variability in SUs geometry, and in particular in the SU bottomset character and offshore extent can be due to three conditions that are not mutually exclusive: 1) substantial increase in the energy regime of along-shore WACC capable of hampering the AMW progradation and thus preventing sediment to reach the bottomset (thin bottomset) (see also Cattaneo et al., 2007). Particularly, during the SU3, which indeed shows the shortest offshore extent, the WACC confined the sediment accumulation mainly in the upper foreset/topset. 2) A second hypothesis consider an unchanged value in current intensity but a subtle shift of the WACC position, toward the shallower regions of the AMW, due to changes in thermohaline properties at seasonal and decadal scales, as documented by oceanographic temporal series (e.g. Vilibić et al., 2013). 3) The third hypothesis considers an increase in the across-shore sediment supply component that controls the clinothem offshore extent, by overwhelming the effect of along shore currents (see Hampson and Storms, 2003; Zhang et al., 2019; Carvajal et al., 2009; Zavala and Arcuri, 2016; Plink-Bjorklund, 2020). In particular, the SU4/5 thick bottomsets correspond to the late period of AMW construction, when the advection favored the bottomset aggradation through sediment resuspension of sediments from the foreset to the bottomset. In addition, in the SU5 case, the relative increased activity of the WACC has been also favored by the fact that Apennine rivers have been partially “chocked” in consequence of the effects of anthropogenic interventions as damming and river harnessing (Palinkas et al., 2005; Stevens et al., 2007).

5.3. Seismic stacking patterns at intra-clinothems scale

The examination of the geometric arrangements of seismic reflectors and bedset terminations highlighted changes in the intra-clinothem stacking patterns during the AMW evoution (Fig. 6b and c). These types of intra-clinothem motifs, which have been largely documented both across modern deltas and also in their ancient counterparts, have been interpreted as the result of the impact of short-term vs long-term sedimentary processes during the mud belt construction (Lobo et al., 2005; Xue et al., 2010; Lee et al., 2005; Peng et al., 2018). We speculate that this different stratal pattern and bedset terminations configuration could be influenced by the short-lived climatic variations, which have dictated secular sediment supply fluctuations of riverine input (see Fanget et al., 2014; Bassetti et al., 2016; Cong et al., 2021). The climate of the Late Holocene in the Mediterranean has been largerly investigated in the last 20 years, highliting, also in the Adriatic region, the presence of centennial-scale hydrological events, that often correspond to wet-dry-wet climatic cycles, where solar irradiance cyclicity and the North Atlantic Oscillation variability have been considered the primary driving mechanisms (Nieto-Moreno et al., 2011). This natural climate variability has the controls on fluvial discharges, erosion in drainage basins as well as hydrodynamic regime of water masses and currents: all these factors influence on the supply, transport and mechanism of deposition of sediment over time (see Piva et al., 2008; Dermody et al., 2012; Siani et al., 2013, Bassetti et al., 2016, Fanget et al., 2014; Goudeau et al., 2015 for a comprehensive review). We do not consider the role played by variations of the accommodation space and oscillations in the sea level to be sufficient controlling factors, that, although not negligible, have values of less than 1 m (see Baker and Haworth, 2000; Siddall et al., 2003; Piva et al., 2008 for sea-level variations during the last HST). Intra-clinotheme difference in bedsets stacking patterns have been higlighted by Pellegrini et al. (2021), where authors show that the different styles of intra-clinotheme arrangement can be linked to events of hyperpycnal flows, storms and bottom currents acting concurrently in the basin. Earlier works also documented a strong interaction between river flood and the effect of along-shelf redistribution, in controlling the resultant intra-clinotheme motif (e.g. Slingerland et al., 2008; Durán et al., 2018; Carlin et al., 2019; Gamberi et al., 2020).

5.4. Role of intra-clinotheme channels in the across-shelf sediment transport

Within mud-prone, shallow-water mudbelt, the presence of fine-

scale elements linked to across-shelf sediment flows has been reported rarely, and generally, the few, documented examples come from ancient systems (see Pattison et al., 2007; Hampson, 2010; Zhang et al., 2017; Li and Schieber, 2018). However, several studies have demonstrated that sustained hyperpycnal flows can develop also across gently sloped shelves, as the case of the Adriatic inner shelf (Winterwerp, 2006; Van Rijn, 2007).

Our hypothesis that the V-shaped incisions found within SU1 and SU2 are shallow-water channels formed during the AMW early stages, and linked to riverine processes, is supported by their architectural arrangement, as they seem to develop all along the foreset (with single- and multi-storey incisions) coupled with the presence of lobated-shape deposits at the bottomset. In the AMW, this arrangement, i.e. cut-and-fill features, and distributary channels with associated terminal lobe has been documented also in the modern Po delta by high-resolution seismic and bathymetric surveys (Correggiari et al., 2005; Bosman et al., 2020). More in general, sustained flows that can bypass the coastal areas during river floods are necessary to form topset to foreset channel pathways, even without the presence of a high-slope angle or high sediment concentrations (Lamb et al., 2010). The presence of these channel features, oriented perpendicular to the coast dip, and that reach water depths up to 55–60 m, at distance up to 15 km from the coastline, let us speculate that their origin could be mainly related to riverine activity (e.g. Oliaru and Bhattacharya, 2006; Pattison et al., 2007; Xiong et al., 2023). Hyperpycnal-aided mud flows are in fact capable to cross-shelf transport of suspended sediments to advance far beyond the coastline, especially if they are generated by “dirty river systems”, i.e. those small mountainous rivers capable of very high discharge rates, draining high-relief terrains (Mulder and Syvitski, 1995; Johnson et al., 2001). The relatively small, Apennine rivers represent sediment delivery systems which provide a sediment flux disproportionate to their size, due to steep gradients associated with the smaller watersheds of tectonically active regions such as the Apennine chain (Milliman and Syvitski, 1992; Syvitski and Kettner, 2007; Milliman and Farnsworth, 2011). During the last century, dam construction, river stabilization, and quarrying have altered the discharge of Apennine rivers and reduced the amount of sediment load delivered to the Adriatic Sea (Acciarri et al., 2016). However, in pre-dam conditions, Apennine rivers were capable of freely discharging considerable quantities of sediments which were likely to generate hyperpycnal discharge across the AMW (see Milliman and Syvitski, 1992; Farroni et al., 2002; Borrelli et al., 2014; Pellegrini et al., 2021). Moving from older to more recent SUs, channels gradually decrease in size, extent, and recognizability. In SU4, and especially SU5, channel-like features are only present within U-shaped erosional surfaces on the topset, which resemble the features that have been documented by Bosman et al. (2020) in the Po prodelta system (Fig. 7c). We speculate that the lowering of the receiving shelf’s relative water depth as a result of the AMW growth, along with the damming and utilization of Appennine rivers over the past century, can account for the decline in the distance covered by the channel-like features.

5.5. Ancient and modern analogues to AMW

There have been many different genetic interpretations of the evidence of submarine channelization within inner-shelf, shallow-water successions, including variations in the depositional environments, the position of sea level, and the sea-level curve (i.e. e. high-versus low-stand). Channelization in delta and prodelta front has been largely documented in coarse-grained, Gilbert-type deltas, whereas, in low-angle, fine-grained settings, the evidence are lower (e.g. Olariu and Bhattacharya, 2006). The presence of marine mudstone-encased sandstone/heterolitc bodies linked to across-shelf sediment transport has been identified along the outcrops of Devonian-Cretaceous Western Interior Seaway of North America and Canada, within ancient mud-prone, shallow-water mudbelts (Pattison et al., 2007; Varban and Plint, 2008; Soyinka and Slatt, 2008; Bhattacharya and MacEachern, 2009; Hampson, 2010; Wilson and Schieber, 2014; Hampson and Premwichein, 2017; Li and Schieber, 2018). The many studies conducted on the isolated clusters of shelfal-channels in the Blackhawk Formation (Book Cliffs, USA) among all the pertinent and comparable systems, indicate that the formation of a shallow-water, across-shelf transport component can occur even in an environment that shows a remarkable resemblance to the Western Adriatic Shelf (see Pattison et al., 2007; Pattison and Hoffman, 2008) (Fig. 10). In particular, the detached sand bodies in the Kenilworth Member suggests that channelized bodies occur also during the HST and are not solely restricted to the low stand and falling stage systems tracts. The deltaic clinoforms formed on the shelf (or shallow ramp) of the Rock Springs Formation (Lower Campanian of Western Interior Seaway), and of the Battfjellet Formation (Eocene Central Basin of Spitsbergen), where progradation was primarily driven by deposition from weak hyperpycnal flow turbidity currents (Plink-Bjorklund, 2020). Discrete intervals of large scours interpreted as the result of the erosional activity of flows linked to high-discharging fluvial events and storms have been reported also from the Devonian Lower Gennesse Group (Wilson and Schieber, 2014).

Among the examples from the modern systems are Syvitski and Farrow (1989), who worked on the bayhead prodelta and showed how high-density hyperpycnal flows can be generated on fine-grained delta fronts. These flows have the ability to cut subaqueous channels and transport sand into the prodelta region. Similarly, in the fine-grained Huanghe delta, high-density flows have been suggested to be the cause of channel cutting and sediment transport into very-shallow waters (Wright et al., 1986); finally, in the tide-dominated Han River Delta, where the 40–50 m high highstand delta clinothems are channelized by tidal channels in the innermost 30 km (Cummings et al., 2016).

6. Conclusions

Through the interpretation of very high-resolution CHIRP profiles, the Late Holocene Adriatic Mud Wedge (AMW) along the Western Adriatic Sea was analyzed. This analysis resulted in the identification of AMW stacking patterns and small-scale geomorphic architectural elements, such as foreset channels and lobes, that are generally thought to be uncommon in this type of environment. The internal architecture of AMW exhibits variations in intra-clinothem stacking patterns of the bedset-termination migrations as well as alternating complex geometries (thin vs. thick bottomset). e. brief) that suggest a complex history in which the system seems to be impacted by changes in the oceanographic regime and sediment supply.

The AMW internal architecture shows alternations of the complex geometries (thin vs thick bottomset), and the difference in composite stacking patterns (i.e. short-lived phases of intra-clinothem bedset migrations) that are indicative of a complex history, where the system appears influenced by the fluctuations in the sediment supply and oceanographic regime interaction.

Specifically, it appears clear that the riverine-linked sediment supply regime gradually decreases over time, giving way to a redistribution of sediment via stronger along-shore currents. The primary evidence is the gradual shift from the foreset channels of the older Sus, to the smaller-scale forms of the late AMW stages, which are mostly restricted to the topset region. This evolution is coupled with the transition from localized deposition in front of the mouths of the main Apennine rivers of the older SUs, to more smoothed and uniform depocentres distributed along the coast of the younger SUs. This implies that in the early stages, the sedimentary “linking” between the topset and the bottomset of the AMW was guaranteed through sedimentary pathways created by fluvial sediment and carried offshore throughout riverine hyperpycnal flows. By contrast, in the later stages, most of the sediments remain trapped in the topset/upper foreset sectors, where they are heavily reworked, as the presence of erosional surfaces seem to indicate, and finally redistributed along the coast and toward the offshore by along-shore currents.

Our results imply that, despite the apparent AMW homogeneity at

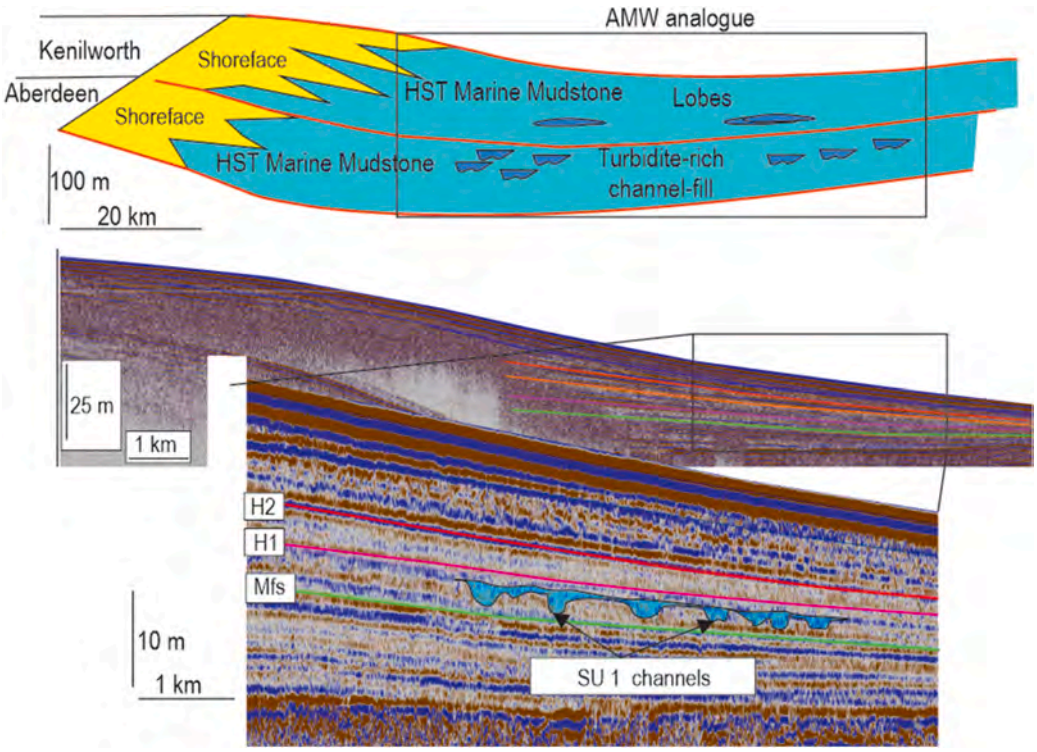

Fig. 10. Schematic cross-section oriented along the depositional dip of the Campanian Aberdeen/Kenilworth shelf-system (Book Cliffs, Utah, USA) (modified from Pattison et al., 2007) used as a comparison with the shallow-water, inner-shelf channelization of the AMW. Key dissimilarities include the substantial diversities in the Book Cliff channels horizontal scale, which is an order of magnitude lower than the systems found in the AMW, and the nature of the channel infill, which is virtually unknown in the AMW.

the regional scale, m-scale, lateral, and vertical heterogeneities are formed due to the complex bedset terminations stacking patterns and the presence of channels, lobes and the large erosional surfaces along topset and the foreset. Low-resolution datasets associated with these types of environments require consideration of these factors, as they can alter the exploration and exploitation estimates for shallow water, mudbelt-linked reservoirs.

CRediT authorship contribution statement

Giacomo Dalla Valle: Conceptualization, Investigation, Methodology, Writing – original draft, Writing – review & editing. **Marzia Rovere:** Investigation, Methodology, Visualization, Writing – review & editing. **Claudio Pellegrini:** Conceptualization, Methodology, Validation, Writing – review & editing. **Fabiano Gamberi:** Conceptualization, Investigation, Methodology, Writing - review & editing.

Declaration of competing interest

The authors declare that they have no known competing financial interests or personal relationships that could have appeared to influence the work reported in this paper.

Data availability

The data that has been used is confidential.

References

Acciarri, A., Bisci, C., Cantalamessa, G., Di Pancrazio, G., 2016. Anthropogenic influence on recent evolution of shoreline between the Conero Mt. and the Tronto R. mouth (southern Marche. Central Italy). Catena 147, 545–555. https://doi.org/10.1016/j.catena.2016.08.018.

Alexander, C.R., DeMaster, D.J., Nittrouer, C.A., 1991. Sediment accumulation in a modern epicontinental-shelf setting: the Yellow Sea. Mar. Geol. 98, 51–72.

Artegiani, A., Bregant, D., Paschini, E., Pinardi, N., Raicich, F., Russo, A., 1997. The adriatic seageneral circulation. Part II: baroclinic circulation structure. J. Phys. Oceanogr. 27, 1515–1532.

Baker, R., Haworth, R.J., 2000. Smooth or oscillating late Holocene sea-level curve? Evidence from the palaeo-zoology of fixed biological indicators in east Australia and beyond. Mar. Geol. 163, 367–386.

Bassetti, M.A., Berné, S., Sicre, M.A., et al., 2016. Holocene hydrological changes of the Rhone River (NW Mediterranean) as recorded in the marine mud belt. Clim. Past 12, 1539–1553.

Bernè, S., Jouet, G., Bassetti, M.A., Dennielou, B., Taviani, M., 2007. Late Glacial to Preboreal sea-level rise recorded by the Rhone deltaic system (NW Mediterranean). Mar. Geol. 245, 65–88.

Bhattacharya, J.P., MacEachern, J.A., 2009. Hyperpycnal rivers and prodeltaic shelves in the cretaceous Seaway of North America. J. Sediment. Res. 79, 184–209.

Borrelli, P., Märker, M., Panagos, P., Schütt, B., 2014. Modeling soil erosion and river sediment yield for an intermountain drainage basin of the Central Apennines, Italy. Catena 114, 45–58, 2014.

Bosman, A., Romagnoli, C., Madricardo, F., Correggiari, A., Remia, A., Zubalich, R., Fogarin, S., Kruss, A., Trincardi, F., 2020. Short-term evolution of Po della Pila delta lobe from time lapse high-resolution multibeam bathymetry (2013–2016). Estuar. Coast Shelf Sci. 233, 106533.

Carlin, J., Addison, J., Wagner, A., Schwartz, V., Hayward, J., Severin, V., 2019. Variability in shelf sedimentation in response to fluvial sediment supply and coastal erosion over the Past 1,000 years in Monterey Bay, CA, United States. Front. Earth Sci. 7, 113. https://doi.org/10.3389/feart.2019.0011.

Carvajal, C., Steel, R., Petter, A., 2009. Sediment supply: the main driver of shelf-margin growth. Earth Sci. Rev. 96, 221–248.

Cattaneo, A., Correggiari, A., Langone, L., Trincardi, F., 2003. The late Holocene Gargano subaqueous delta, Adriatic shelf: sediment pathways and supply fluctuations. Mar. Geol. 193, 61–91.

Cattaneo, A., Trincardi, F., Langone, L., Asioli, A., Puig, P., 2004. Clinoform generation on Mediterranean margins. Oceanography 174, 104–111.

Cattaneo, A., Trincardi, F., Asioli, A., Correggiari, A., 2007. The western Adriatic shelf clinoform: energy-limited bottomset. Continent. Shelf Res. 27, 506–525.

Cong, J., Hu, G., Jonell, T.N., Zhang, Y., Li, Y., Bi, S., 2021. Source-to-sink and evolutionary processes of the East China Sea inner-shelf mud belt and its response to environmental changes since the Holocene: New evidence from the distal mud belt. Holocene 31, 1071–1088.

Correggiari, A., Cattaneo, A., Trincardi, F., 2005. Depositional patterns in the Late-Holocene Po delta system. In: Bhattacharya, J.P., Giosan, L. (Eds.), Cocepts, Models and Examples, vol. 83. SEPM Spec. Pubbl., pp. 365–392

Cummings, D.I., Dalrymple, R.W., Choi, K., Jin, J.H., 2016. The Tide Dominated Han River Delta, Korea, vols. 1–5. Elsevier, Amsterdam. https://doi.org/10.1016/b978-0-12-800768-6.00001-8.

Dermody, B.J., de Boer, H.J., Bierkens, M.F.P., Weber, S.L., Wassen, M.J., Dekker, S.C., 2012. A seesaw in Mediterranean precipitation during the Roman period linked to millennial-scale changes in the north Atlantic. Clim. Past 8, 637–665.
Dıaz, J.I., Palanques, A., Nelson, C.H., Guillen, J., 1996. Morpho-structure and sedimentology of the Holocene Ebro prodelta mud belt (northwestern Mediterranean Sea). Continent. Shelf Res. 16, 435–456.
Drexler, T.M.A., Nittrouer, C.A., 2008. Stratigraphic signatures due to flood deposition near the Rhone river: gulf of lions, northwest Mediterranean Sea. Continent. Shelf Res. 28, 1877–1894.
Durán, R., Lobo, F.J., Ribó, M., García, M., Somoza, L., 2018. Variability of shelf growth patterns along the iberian mediterranean margin: sediment supply and tectonic influences. Geosciences 8, 168.
Ehrmann, W., Schmiedl, G., Seidel, M., Krüger, S., Schulz, H., 2016. A distal 140 kyr sediment record of Nile discharge and East African monsoon variability. Clim. Past 12, 713–727.
Fanget, A.S., Berné, S., Jouet, G., Bassetti, M.A., Dennielou, B., Maillet, G.M., Tondut, M., 2014. Impact of relative sea level and rapid climate changes on the architecture and lithofacies of the Holocene Rhone subaqueous delta (Western Mediterranean Sea), Sediment. Geol. 305, 35–53.
Farroni, A., Magaldi, D., Tallini, M., 2002. Total sediment transport by the rivers of Abruzzi (Central Italy): prediction with the RAIZAL model. Bull. Eng. Geol. Environ. 61, 121–127. https://doi.org/10.1007/s100640100127.
Gamberi, F., Pellegrini, C., Dalla Valle, G., Scarponi, D., Bohacs, K., Trincardi, F., 2020. Compound and hybrid clinothems of the last lowstand Mid-Adriatic Deep: processes, depositional environments, controls and implications for stratigraphic analysis of prograding systems. Basin Res. 32, 363–377.
Goudeau, M.L.S., Reichart, G.J., Wit, J.C., de Nooijer, L.J., Grauel, A.L., et al., 2015. Seasonality variations in the central mediterranean during climate change events in the late Holocene. Palaeogeogr. Palaeoclimatol. Palaeoecol. 418, 304–318.
Hampson, G.J., 2010. Sediment dispersal and quantitative stratigraphic architecture across an ancient shelf. Sedimentology 57, 96–141.
Hampson, G.J., Premwichein, K., 2017. Sedimentologic character of ancient muddy subaqueous-deltaic clinoforms: down Cliff clay member, bridport sand formation, wessex basin, UK. J. Sediment. Res. 87 (9), 951–966.
Hampson, G.J., Storms, J.E., 2003. Geomorphological and sequence stratigraphic variability in wave-dominated, shoreface-shelf parasequences. Sedimentology 50, 667–701.
Harris, C.K., Sherwood, C., Signell, R.P., Bever, A.J., Warner, J.C., 2008. Sediment dispersal in the northwestern Adriatic Sea (2008). J. Geophys. Res. Ocean 113. https://doi.org/10.1029/2006JC003868.
Hernández-Molina, F.J., Somoza, L., Rey, J., Pomar, L., 1994. Late Pleistocene–Holocene sediments on the Spanish continental shelves: model for very high-resolution sequence stratigraphy. Mar. Geol. 120, 129–174.
Jaeger, J.M., Nittrouer, C.A., 1999. Sediment deposition in an Alaskan fjord; controls on the formation and preservation of sedimentary structures in Icy Bay. J. Sediment. Res. 69, 1011–1026.
Johnson, K.S., Paull, C.K., Barry, J.P., et al., 2001. A decadal record of underflows from a coastal river into the deep sea. Geology 29, 1019–1022.
Kettner, A.J., Syvitski, J.P.M., 2008. Predicting discharge and sediment flux of the Po river, Italy since the late glacial maximum. In: de Boer, P.L., Postma, G., van der Zwan, C.J., Burgess, P.M., Kukla, P. (Eds.), Analogue and Numerical Forward Modelling of Sedimentary Systems: from Understanding to Prediction, vol. 40. IAS Spec. Publ, Oxford, UK, pp. 171–189.
Lamb, M.P., McElroy, B., Kopriva, B., Shaw, J., Mohrig, D., 2010. Linking river-flood dynamics to hyperpycnal-plume deposits: experiments, theory, and geological implications. GSA Bulletin 122, 1389–1400.
Lee, S.H., Lee, H.J., Jo, H.R., Bahk, J.J., Chu, Y., 2005. Complex sedimentation of the Holocene mud deposits in aria-type coastal area, eastern Korea Strait. Mar. Geol. 214, 389–409.
Li, Z., Schieber, J., 2018. Detailed facies analysis of the upper cretaceous tununk shale member, henry mountains region, Utah: implications for mudstone depositional models in epicontinental seas. Sediment. Geol. 364, 141–159.
Liu, J.P., Xue, Z., Ross, K., Wang, H.J., Yang, Z.S., Li, A.C., Gao, S., 2009. Fate of sediments delivered to the sea by Asian large rivers: long-distance transport and formation of remote alongshore clinothems. Sediment. Rec. 7 (4), 4–9.
Lobo, F.J., Herndandez-Molina, F.J., Somoza, L., Dıaz del Rıo, V., Dias, J.M.A., 2002. Stratigraphic evidence of an upper Pleistocene TST to HST complex on the Gulf of Cadiz continental shelf (south-west Iberian Peninsula). Geo Mar. Lett. 22, 95–107.
Lobo, F.J., Dias, J.M.A., Hernandez-Molina, F.J., Gonzalez, R., Fernandez-Salas, L.M., Diaz del Rio, V., 2005. Late Quaternary shelf-margin wedges and upper slope progradation in the Gulf of Cadiz margin (SW Iberian Peninsula). Geological Society Spec.Publ. 244, 7-25.
Martin, J.M., Zhang, J., Shi, M.C., Zhou, Q., 1993. Actual flux of the Huanghe (Yellow river) sediment to the western pacific ocean. Neth. J. Sea Res. 31, 243–254.
Martorelli, E., Falcini, F., Salusti, E., Chiocci, F.L., 2010. Analysis and modeling of contourite drifts and contour currents off promontories in the Italian Sea (Mediterranean Sea). Mar. Geol. 278, 19–30.
Milliman, J.D., Farnsworth, K.L., 2011. River Discharge to the Coastal Ocean: A Global Synthesi. Cambridge University Press, UK., p. 384
Milliman, J.D., Syvitski, J.P.M., 1992. Geomorphic/tectonic control of sediment discharge to the ocean: the importance of small mountainous rivers. J. Geol. 100, 525–544.
Mulder, T., Syvitski, J.P.M., 1995. Turbidity currents generated at river mouths during exceptional discharges to the world oceans. J. Geol. 103, 285–299.
Niedoroda, A.W., Reed, C.W., Das, H., Fagherazzi, S., Donoghue, J.F., Cattaneo, A., 2005. Analyses of a large-scale depositional clinoformal wedge along the Italian Adriatic coast. Mar. Geol. 222, 179–192.
Nieto-Moreno, V., Martinez-Ruiz, F., Giralt, S., et al., 2011. Tracking climate variability in the western Mediterranean during the Late Holocene: a multiproxy approach. Clim. Past 7, 1395–1414.
Olariu, C., Bhattacharya, J.P., 2006. Terminal distributary channels and delta front architecture of river-dominated delta systems. J. Sediment. Res. 76, 212–233.
Oldfield, F., Asioli, A., Accorsi, C.A., Mercuri, A.M., Juggins, S., Langone, L., Rolph, T., Trincardi, F., Wolff, G., Gibbs, Z., Vigliotti, L., Frignani, M., Van der post, K., Branch, N., 2003. A high-resolution late Holocene palaeoenvironmental record from the central Adriatic Sea. Quat. Sci. Rev. 22, 319–342.
Palinkas, C.M., Nittrouer, C.A., 2006. Modern sediment accumulation on the Po shelf, Adriatic Sea. Continent. Shelf Res. 27, 489–505.
Palinkas, C.M., Nittrouer, C.A., 2007. Clinoform sedimentation along the apennine shelf, Adriatic Sea. Mar. Geol. 234, 245–260.
Palinkas, C.M., Nittrouer, C., Wheatcroft, R., Langone, L., 2005. The use of 7Be to identify event and seasonal sedimentation near the Po River delta, Adriatic Sea. Mar. Geol. 222, 95–112.
Patruno, S., Helland-Hansen, W., 2018. Clinoforms and clinoform systems: review and dynamic classification scheme for shorelines, subaqueous deltas, shelf edges and continental margins. Earth Sci. Rev. 185, 202–233.
Patruno, S., Hampson, G.J., Jackson, C.A.-L., 2015. Quantitative characterization of deltaic subaqueous clinoforms. Earth Sci. Rev. 142, 79–119.
Pattison, S.A.J., Hoffman, T.A., 2008. Sedimentology, architecture, and origin of shelf turbidite bodies in the Upper Cretaceous Kenilworth Member, Book Cliffs, Utah, U.S. A. In: Recent Advances in Models of Siliciclastic Shallow-Marine Stratigraphy. SEPM Spe. Publ. 90, pp. 391–420.
Pattison, S.A.J., Bruce Ainsworth, R., Hoffman, T.A., 2007. Evidence of across-shelf transport of fine-grained sediments: Turbidite-filled shelf channels in the Campanian Aberdeen member, book cliffs, Utah, USA. Sedimentology 54, 1033–1064.
Pellegrini, C., Maselli, V., Cattaneo, A., Piva, A., Ceregato, A., Trincardi, F., 2015. Anatomy of a compound delta from the post-glacial transgressive record in the Adriatic Sea. Mar. Geol. 362, 43–59.
Pellegrini, C., Patruno, S., Helland-Hansen, W., Steel, R., Trincardi, F., 2020. Clinoforms and clinothems: fundamental elements of basin infill. Basin Res. 32, 187–205.
Pellegrini, C., Tesi, T., Schieber, J., Bohacs, K.M., Rovere, M., Asioli, A., Trincardi, F., 2021. Fate of terrigenous organic carbon in muddy clinothems on continental shelves revealed by stratal geometries: insight from the Adriatic sedimentary archive. Global Planet. Change 103539.
Peng, Y., Steel, R.J., Rossi, V.M., Olariu, C., 2018. Mixed-energy process interactions read from a compound-clinoform delta (paleo–orinoco Delta, Trinidad): preservation of river and tide signals by mud- induced wave damping. J. Sediment. Res. 88, 75–90.
Piva, A., Asioli, A., Trincardi, F., Schneider, R.R., Vigliotti, L., 2008. Late-Holocene climate variability in the Adriatic Sea (Central Mediterranean). Holocene 18, 153–167.
Plink-Bjorklund, P., 2020. Shallow-water deltaic clinoforms and process regime. Basin Res. 32, 251–262.
Poulain, P.M., 2001. Adriatic Sea surface circulation as derived from drifter data between 1990 and 1999. J. Mar. Syst. 29, 3–32.
Poulain, P.M., Cushman-Roisin, B., 2001. Chapter 3 Circulation. In: Physical Oceanography of the Adriatic Sea. Kluwer Academic Publisher, Dordrecht, the Netherlands, pp. 67–109, 2001.
Revel, M., Ducassou, E., Grousset, F., Bernasconi, S.M., Migeon, S., Revillon, S., Mascle, J., Murat, A., Zaragosi, S., Bosch, D., 2010. 100,000 Years of African monsoon variability recorded in sediments of the Nile margin. Quat. Sci. Rev. 29, 1342–1362.
Siani, G., Magny, M., Paterne, M., Debret, M., Fontugne, M., 2013. Paleohydrology reconstruction and Holocene climate variability in the South Adriatic Sea. Clim. Past 9, 499–515.
Siddall, M., Rohling, E.J., Almogi-Labin, A., Hemleben, C., Meischner, D., Schmelzer, I., Smeed, D.A., 2003. Sea-level fluctuations during the last glacial cycle. Nature 423, 853–858.
Slingerland, R., Driscoll, N.W., Milliman, J.D., Miller, S.R., Johnstone, E.A., 2008. Anatomy and growth of a Holocene clinothem in the Gulf of Papua. J. Geophys. Res. Earth Surf.v. 113.
Soyinka, O.A., Slatt, R.M., 2008. Identification and micro-stratigraphy of hyperpycnites and turbidites in cretaceous Lewis shale, Wyoming. Sedimentology 55, 1117–1133.
Stevens, A.W., Wheatcroft, R.A., Wiberg, P.L., 2007. Seabed properties and sediment erodibility along the western Adriatic margin. Italy. Cont. Shelf Res. 27, 400–416.
Syvitski, J.P.M., Farrow, G.E., 1989. Fjord sedimentation as an analogue for small hydrocarbon-bearing fan deltas. In: Whateley, M.K.G., Pickering, K.T. (Eds.), Deltas: Sites and Traps for Fossil Fuels, vol. 41. Geol. Soc. London, Spec. Publ., pp. 21–43
Syvitski, J.P.M., Kettner, A., 2007. On the flux of water and sediment into the Northern. Adriatic. Continent. Shelf Res. 27, 296–308.
Traykovski, P., Wiberg, P.L., Geyer, W.R., 2007. Observations and modeling of wave-supported sediment gravity flowson the Po prodelta and comparison to prior observations from the Eel Shelf. Continent. Shelf Res. 27, 375–399.
Trincardi, F., Correggiari, A., Roveri, M., 1994. Late Quaternary transgressive erosion and deposition in a modern epicontinental shelf: The Adriatic Semi-enclosed Basin. Geo Mar. Lett. 14, 41–51.
Trincardi, F., Cattaneo, A., Correggiari, A., 2004. Mediterranean prodelta systems: Natural evolution and human impact investigated by EURODELTA. Oceanography 17, 34–45.

Trincardi, F., Campiani, E., Correggiari, A., Foglini, F., Maselli, V., Remia, A., 2014. Bathymetry of the Adriatic Sea: The legacy of the last eustatic cycle and the impact of modern sediment dispersal. J. Maps 10, 151–158.
Urgeles, R., Cattaneo, A., Puig, P., Liquete, C., De Mol, B., Amblàs, D., Trincardi, F., 2011. A review of undulated sediment features on Mediterranean prodeltas: distinguishing sediment transport structures from sediment deformation. Mar. Geophys. Res. 32, 49–69.
Van Rijn, L.C., 2007. Unified view of sediment transport by currents and waves. I: initiation of motion, bed roughness, and bed load transport. J. Hydrol. Eng. 133, 649–667.
Van Wagoner, J.C., Posamentier, H.W., Mitchum, R.M., Vail, P.R., Sarg, J.F., Loutit, T.S., Hardenbol, 1988. An overview of sequence stratigraphy and key definitions. In: Wilgus, C.W., et al. (Eds.), Sea Level Changes: an Integrated Approach, vol. 42. SEPM Special publ, pp. 39–45.
Varban, B.L., Plint, A.G., 2008. Palaeoenvironments, palaeogeography, and physiography of a large, shallow, muddy ramp: Late Cenomanian-Turonian Kaskapau Formation, Western Canada foreland basin. Sedimentology 55, 201–233.
Vigliotti, L., Verosub, K., Cattaneo, A., Trincardi, F., Asioli, A., Piva, A., 2008. Palaeomagnetic and rock magnetic analysis of Holocene deposits from the Adriatic Sea: detecting and dating short-term fluctuations in sediment supply. Holocene 18, 141–152.
Vilibić, I., Šepić, J., Proust, N., 2013. Weakening of thermohaline circulation in the Adriatic Sea, Clim. Res, 55, 217–225.
Walsh, J.P., Nittrouer, C.A., Palinkas, C.M., Ogston, A.S., Sternberg, R.W., Brunskill, G.J., 2004. Clinoform mechanics in the Gulf of Papua, New Guinea. Continent. Shelf Res. 24, 2487–2510.
Warrick, J.A., 2020. Littoral sediment from rivers: Patterns, rates and processes of river mouth morphodynamics Front. Earth Sci. 8, 355.
Wilson, R.D., Schieber, J., 2014. Muddy prodeltaic hyperpycnites in the Lower Genesee Group of Central New York, USA: implications for mud transport in epicontinental seas. J. Sediment. Res. 84, 866–874.
Winterwerp, J.C., 2006. Stratification effects by fine suspended sediment at low, medium and very high concentrations. J. Geophys. Res. 111, C5. https://doi.org/10.1029/2005JC003019.
Wright, L.D., Coleman, J.M., 1973. Morphology of major river deltas as functions of ocean wave and river discharge regimes. AAPG Bull. 57, 370–398.
Wright, L.D., Yang, Z.S., Bornhold, B.D., Keller, G.H., Prior, D.B., Wiseman, W.J., 1986. Hyperpycnal plumes and plume fronts over the Huanghe (Yellow River) delta front. Geo Mar. Lett. 6, 97–10.
Xiong, H., Zhang, Z., Lu, B., Zong, Y., Wu, J., 2023. Evolution of the first mouth bar, distributaries and floodplains of the Pearl River Delta. Geomorphology 431, 108690.
Xu, K.H., Li, A., Liu, J.P., Milliman, J.D., Yang, Z.S., Liu, C.S., Kao, S.J., Wan, S.M., Xu, F. J., 2012. Provenance, structure, and formation of the mud wedge along inner continental shelf of the East China Sea: a synthesis of the Yangtze dispersal system. Mar. Geol. 291, 176–191.
Xue, Z., Liu, J.P., De Master, D., Van Nguyen, L., Ta, T.K.O., 2010. Late Holocene evolution of the Mekong subaqueous delta, southern Vietnam. Mar. Geol. 269, 46–60.
Zavala, C., Arcuri, M., 2016. Intrabasinal and extrabasinal turbidites: origin and distinctive characteristics. Sediment. Geol. 337, 36–54.
Zhang, J., Steel, R., Ambrose, W., 2017. Paleocene Wilcox cross-shelf channel-belt history and shelf-margin growth: key to Gulf of Mexico sediment delivery. Sediment. Geol. 362, 53–65.
Zhang, K., Li, A., Huang, P., Lu, J., Liu, X., Zhang, J., 2019. Sedimentary responses to the cross-shelf transport of terrigenous material on the East China Sea continental shelf. Sediment. Geol. 384, 50–59.